

CLINICAL APPLICATIONS OF MEYER'S LOOP TRACTOGRAPHY

CRISTINA GOGA¹, IOAN ȘTEFAN FLORIAN², MENA RUBEN RODRIGUEZ³, ZEYNEP FIRAT⁴,
IOANA HĂLMACIU⁵, KLARA BRÎNZANIUC⁶

^{1,5,6}University of Medicine and Pharmacy Tîrgu-Mureș, ^{1,2}“Iuliu Hațieganu” University of Medicine and Pharmacy Cluj Napoca,
^{1,3,4}Yeditepe University School of Medicine Istanbul, Turkey

Keywords: Meyer's loop; diffusion tensor tractography; diffusion tensor imaging; epilepsy; visual field defect

Abstract: Visual field defects (VFD) due to Meyer's loop injury may occur after temporal lobe resection surgery. Diffusion tensor tractography (DTT) of the Meyer's loop may reduce the risk of postoperative VFD. Currently, there is no standardized method to perform tractography for this structure. We performed DTT of the Meyer's loop in 10 healthy subjects and demonstrated the complex arrangement of the various projection fibers that compose the Meyer's loop and the complex relations with the neighbouring fiber systems. Evaluation of the Meyer's loop through the use of tractography may be a useful method to predict VFD after temporal resection surgery and this anatomical knowledge may be used to build surgical strategies and tactics to avoid the risk of intraoperative damage to this structure.

Cuvinte cheie: ansa Meyer, tractografie, rezonanță magnetică nucleară de difuziune, epilepsie, defecte de câmp vizual

Rezumat: Defectele de câmp vizual (DCV) datorate leziunilor ansei Meyer pot să apară după rezecțiile chirurgicale ale lobului temporal. Tractografia (DTT, Diffusion Tensor Tractography) ansei Meyer ar putea reduce riscul de apariție al DCV postoperatorii. În prezent, nu există o metodă standardizată pentru realizarea tractografiei acestei structuri. Am realizat DTT pentru ansa Meyer la 10 subiecți umani sănătoși și am demonstrat aranjamentul complex al variatelor fibre de protecție care compun ansa Meyer și relațiile complexe cu sistemele de fibre adiacente. Evaluarea ansei Meyer prin tractografie ar putea reprezenta o metodă utilă pentru a prezice DCV după rezecțiile chirurgicale ale lobului temporal și aceste cunoștințe anatomice ar putea fi utilizate pentru a dezvolta strategii chirurgicale și tactici, care permit evitarea riscului de a leza intraoperator această structură importantă.

INTRODUCTION

Selective amygdalohippocampectomy and temporal lobe resections as surgical treatments for mesial temporal lobe epilepsy are well established methods. A common finding after all types of temporal resections is postoperative VFD caused by intraoperative damage to the Meyer's loop. Although, Meyer's loop is commonly known as the temporal loop of the anterior fibers of the optic radiation, recent studies have shown that various other projection fibers for the temporal and occipital regions participate in the formation of this loop, including the optic radiation.(1-4) DTT has important clinical applications in neurosurgery including preoperative planning and intraoperative identification of individual white matter fiber systems. Tractography of the Meyer's loop may predict the probability of the VFDs after temporal lobe resections and reduce the risk of intraoperative injury.

Tractography, or DTT is the advanced magnetic resonance imaging (MRI) technique that allows for a 3-dimensional reconstruction and analysis of important individual white matter fiber systems. DTT images are generated starting from the information offered by diffusion tensor imaging (DTI). DTI is a MRI technique that can be used to evaluate the directionality of the diffusion of water molecules as they move between the white matter fibers.(5-7) From this information, the main direction and the extent of water diffusion can be determined, and the orientation of white matter fibers indirectly evaluated. This technique, developed more than a decade ago, provides a unique noninvasive, in vivo, visualization of the white matter architecture. DTT is generated using mathematical algorithms that connect image voxels based on their anisotropy

and principal diffusion direction.(7-10) Because DTT offers the only currently available method for a noninvasive investigation of the white matter fibers, it might provide additional data regarding the anatomy of the Meyer's loop.(11-16) Currently, there is no standardized method to perform tractography for Meyer's loop. The angulation of the fibers in the Meyer's loop and complex relations with several neighbouring fiber systems represent challenges for the accurate demonstration of the Meyer's loop, because of distortions and mathematical algorithm errors associated with the delineation of such complex arrangements of white matter fibers.

OBJECTIVES

Below, we provide a description of our DTT technique for Meyer's loop tractography, and discuss the current clinical uses of Meyer's loop tractography and future advances in the field.

METHODS

Ten healthy subjects, without history of neurological disease, head injury, or psychiatric disorder (4 females and 6 males, mean age 36 years, range 16-59 years) were recruited after obtaining institutional board review approval. We performed MRI using a 3.0-T MR unit (Philips, Ingenia, Eindhoven, Netherlands) with an 8-channel sensitivity encoding (SENSE) head coil. DTI was acquired using a single-shot spin echo planar imaging (EPI; TR 3759 ms, TE 95 msec, EPI factor 47, slice thickness 2.5 mm, gap 0 mm). Sixteen diffusion directions at $b=800$ seconds/mm² were acquired in addition to $b=0$ images. Sixty slices were taken for whole brain coverage

¹Corresponding author: Cristina Goga, Str. Ghe. Marinescu, Nr. 38, Tîrgu-Mureș, România, E-mail: gogacristina@gmail.com, Tel: +40744 553455
Article received on 21.10.2014 and accepted for publication on 06.11.2014
ACTA MEDICA TRANSILVANICA December 2014;2(4):187-190

CLINICAL ASPECTS

from the vertex to the foramen magnum. The average acquisition time was 6 minutes. The reconstructed voxel size was 1.75X1.75X2.50 mm. Whole brain T1-weighted 3D turbo field echo (3D T1-TFE), with the same resolution, was acquired in the sagittal plane (TR 9.0 ms, TE 4.2msec, slice thickness 0.9mm) and co-registered for anatomical guidance.

DTI computed fractional anisotropy (FA) maps were individually co-registered with T1-weighted images using the MRI system's workstation (Achieva, Philips, Extended MR Workspace 2.6.3.3). FA maps were displayed as colour-orientation maps. The colour-coding of the white matter fiber tracts in the FA maps was as follows: red for left-right oriented fibers, blue for superior-inferior oriented fibers and green for anterior-posterior oriented fibers.

The fiber tracking software was used to generate DTT. The 3-dimensional fiber systems reconstruction was performed using the FACT (Fiber Assignment by Continuous Tracking) method, which is a deterministic method that initiates fiber trajectories from user-defined voxels or seeds.(7,10) Anisotropy threshold values for FA and deflection parameters were set between 0.27-0.35 and 700-915 (where 0 refers to full deflection and 1000 to no deflection) respectively to obtain the maximum tract conspicuity. A knowledge-based multiple-ROI technique was used.(8,17,18) To delineate the relevant white matter fibers, multiple ROIs were placed in the white matter of the occipital region, and the regions of the lateral geniculate body and the optic tract according to previously described anatomical reference methods to identify the lateral geniculate body and optic tracts in T1-weighted images and color-coded FA images.(19-21) The colors of the reconstructed tracts on DTT were selected to permit optimal visualization. The 3D reconstructed fibers were visualized by superimposition on 3-planar T1-weighted 3D turbo field echo (3D T1-TFE) images to enhance their precise anatomical localization and relationship with other anatomical structures.

Six white matter tracts relevant to the Meyer's loop were reconstructed: the posterior thalamic peduncle that includes the optic radiation, the occipitopontine/ parietopontine fibers, the anterior commissure, the occipitofrontal fasciculus, the uncinate fasciculus and the inferior longitudinal fasciculus. To ensure a comprehensive reconstruction off all possible Meyer's loop fibers, a large ROI in the occipital lobe, defined on a coronal image, and a large ROI in the region of lateral geniculate body, including the pulvinar and crus cerebri of the midbrain, and defined on a sagittal image were used. Then, an exhaustive search was performed to identify all the fibers that penetrate both ROIs and participate in the formation of Meyer's loop, and then parcelate these fibers according to their different connections. After Meyer's loop was identified, a ROI in the frontal lobe, using a coronal image, was placed, in addition to the occipital ROI, to reconstruct the occipitofrontal fasciculus. For reconstructing the fibers of the anterior commissure two ROIs were placed 10 mm apart on the left and right side of the midsagittal plane. The uncinate fasciculus was reconstructed by placing one ROI in the anterior temporal lobe and a second ROI in the white matter of the basal portion of the frontal lobe in the coronal plane.

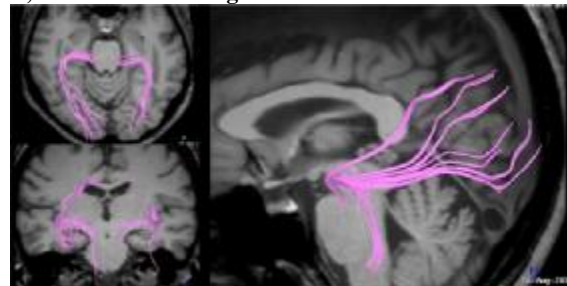
RESULTS

Meyer's loop was reconstructed in all subjects (figure no. 1). Fibers originating in the region of the lateral geniculate body, including pulvinar and the lateral aspect of crus cerebri of the midbrain, extended in an anterolateral direction into the anterior temporal region, before these fibers looped posteriorly and reached the occipital cortical region. This temporal loop is commonly known as the Meyer's loop. All the fibers composing

the Meyer's loop continued their course in the roof of the temporal horn, atrium and occipital horn of the lateral ventricle. In the occipital region, these fibers turned medially, posterior to the occipital horn of the lateral ventricle and reached their cortical terminations. Several projection fibers participated in the formation of the Meyer's loop. Optic radiation fibers originating in the lateral geniculate body and in continuation with the optic tract passed in the Meyer's loop and continued their course towards the occipital visual cortex. The posterior thalamic peduncle includes thalamocortical projection fibers that originate in the pulvinar and connect the pulvinar of the thalamus with occipital cortical regions. The optic radiation is one of the various projection fibers in the posterior thalamic peduncle.

The accurate differentiation between these various posterior thalamic peduncle fibers was extremely difficult, because all these fibers originating either in the lateral geniculate body or in the pulvinar merged and intermingled before forming the Meyer's loop, and could not be distinguished or separated at this level. The occipitopontine fibers, projection fibers originating in the occipital cortex and terminating in the pontine nuclei, coursed in the Meyer's loop together with the optic radiation fibers and thalamocortical projection fibers of the posterior thalamic peduncle. These occipitopontine fibers intermingled with the optic radiation and with the posterior thalamic peduncle fibers, at the level of the Meyer's loop, and then, continued their course in the lateral portion of the crus cerebri of the midbrain to reach the pontine nuclei. All the fibers composing the Meyer's loop continued their course, as part of the sagittal stratum, in the roof of the temporal horn, atrium and occipital horn of the lateral ventricle. In the occipital region, these fibers turned medially, posterior to the occipital horn of the lateral ventricle and reached their cortical terminations.

Figure no. 1. DTT reconstruction of Meyer's loop (pink) in axial, coronal and left sagittal views



The reconstructed fibers have been superimposed on T1-weighted 3D turbo field echo (3D T1-TFE) images to enhance their precise anatomical localization and relationship with other anatomical structures. Fibers originating in the region of the lateral geniculate body, including pulvinar and the lateral aspect of crus cerebri of the midbrain, extended in an anterolateral direction into the anterior temporal region, before these fibers looped posteriorly and reached the occipital cortical region. All the fibers composing the Meyer's loop continued their course in the roof of the temporal horn, atrium and occipital horn of the lateral ventricle, and then these fibers turned medially, posterior to the occipital horn of the lateral ventricle, to reach the occipital cortex.

An intricate relationship of the Meyer's loop with the uncinate fasciculus, occipitofrontal fasciculus, the anterior commissure and the inferior longitudinal fasciculus was demonstrated (figure no. 2).

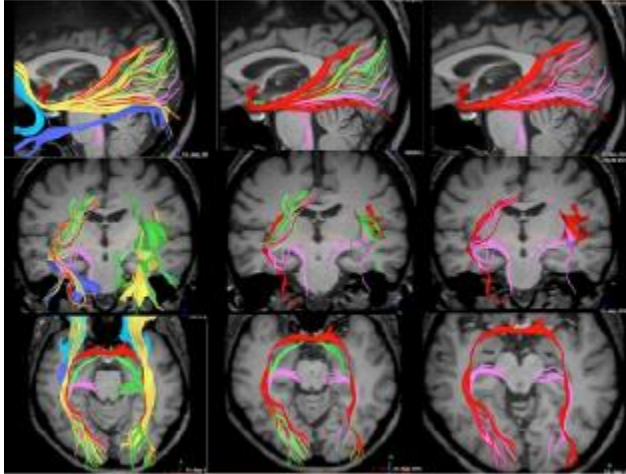
DISCUSSIONS

By using our DTT technique, we were able to demonstrate that several projection fibers system, including optic radiation, posterior thalamic peduncle and occipitopontine fibers participate in the formation of the Meyer's loop. With superimposition of the 3-dimensionally reconstructed fibers on 3-planar T1-weighted 3D turbo field echo (3D T1-TFE) images,

CLINICAL ASPECTS

the composition, course and relations of the Meyer's loop with neighboring fibers could be revealed and evaluated, which could be useful for neurosurgical planning and intraoperative guidance.

Figure no. 2. DTT reconstruction of the complex white matter fiber systems related to Meyer's loop



The reconstructed fibers have been superimposed on T1-weighted 3D turbo field echo (3D T1-TFE) images. *Upper:* Axial view of the reconstructed white matter fibers that intermingle in the region of the Meyer's loop: occipitopontine fibers and posterior thalamic peduncle (pink) that includes optic radiation (green); uncinate fasciculus (light blue); anterior commissure (red); occipitofrontal fasciculus (yellow); inferior longitudinal fasciculus (blue). The optic radiation fibers (green) are in continuation of the optic tract (green). *Middle:* The complex fiber systems related to the Meyer's loop that terminate in the occipital cortex, on a coronal view: occipitopontine fibers and posterior thalamic peduncle (pink); optic radiation (green); anterior commissure (red); occipitofrontal fasciculus (yellow); inferior longitudinal fasciculus (blue). *Lower:* Sagittal view demonstrating the white matter fibers related to Meyer's loop in the anterior temporal region: occipitopontine fibers and posterior thalamic peduncle (pink) that includes optic radiation (green); uncinate fasciculus (light blue); occipitofrontal fasciculus (yellow); anterior commissure (red); inferior longitudinal fasciculus (blue). Occipitofrontal fasciculus together with the lateral extension of the anterior commissure intermingle with the projection fibers in the Meyer's loop to form the sagittal stratum, and reach the occipital cortex. The inferior longitudinal fasciculus joins the inferior border of the sagittal stratum.

Although several studies, using either the extent of temporal resections or fiber dissection technique, investigated the anatomy of the Meyer's loop, there is still considerable disagreement on the precise location, course and anatomic details of the Meyer's loop.(22-35) The anterior limit of the Meyer's loop has not been well established as it has been estimated as anywhere from 20 to 60 mm posterior to the temporal pole, with a tendency to lower the estimates in the more recent studies.(19,36) As a result, presently, the occurrence and extent of a postoperative VFD, owing to injury of the Meyer's loop during surgery for temporal epilepsy, cannot be accurately predicted by conventional MRI methods or by measuring the extent of resection. Only a few DTT studies with very small cohorts have demonstrated that DTT can reconstruct and analyze the Meyer's loop anatomical details.(11,19,37-40) These studies used either deterministic or probabilistic methods to evaluate the anatomical details of the Meyer's loop, by using 2 ROIs, a ROI in the lateral geniculate body and a second ROI in the occipital calcarine cortex, and showed variable results of the locations and course of the Meyer's loop. To the authors knowledge, this is the first study that applied a comprehensive method for reconstruction of all projection fibers that participate in the formation of the Meyer's loop, by using large ROI's, a first ROI in the white matter of the occipital lobe and a second one in the region of the lateral geniculate body, that includes the pulvinar and the lateral portion of the crus cerebri of the mesencephalus. The fact that several projection fibers for the

temporal and occipital regions, including the optic radiation, participate in the formation of the temporal loop might explain the variable and contradictory result of surgical resection studies, that evaluate the location of the Meyer's loop indirectly by establishing the extent of the temporal lobe resections and therefore of the Meyer's loop. The presence of other projection fibers involved in the Meyer's loop might explain why larger resection sizes is not consistently accompanied by a VFD, as the resected fibers in the Meyer's loop were not the optic radiation fibers, but the various other projection fibers, with an unknown functional impact.

DTT of the Meyer's loop, prior to temporal lobe resection or selective amygdalohippocampectomy, may reduce the risk of postoperative VFD. Taoka and coworkers used a preoperative DTT of the Meyer's loop and found a significant correlation of the postoperative VFDs with the extension of surgical resection beyond the anterior limit of the Meyer's loop, where there was no correlation with the extent of resection of the temporal lobe.(16) Similarly, Chen and coworkers found that postoperative VFD could be predicted from the grade of injury of the Meyer's loop measured by pre and intra-operative DTT in patients having temporal lobe resections.(37) Both these DTT studies demonstrated an important variability of the anterior extension of Meyer's loop, but the exact location of the anterior fibers of the Meyer's loop and their relationship to the temporal pole remains controversial. However, with DTT it might be able to estimate the location of the optic radiation fibers at the level of the Meyer's loop, based on the correlation of the VFD with the extent of resection of the Meyer's loop that is not possible with dissection studies or older studies based on intraoperative estimates. Dissection studies cannot differentiate individual optic radiation fibers, while older studies using intraoperative estimates of resection size that assume the occurrence of VFDs correlates with the resection size that is questioned by this recent DTT studies.

The ultimate anatomy of Meyer's loop requires future studies by using a combination of cadaveric white matter fiber dissection, histological-tracing studies that are applicable in humans and DTT. Our observations from DTT, are based on a population of 10 healthy subjects, and future work, on larger populations, and by comparing different deterministic and probabilistic algorithms are required to validate our results. Patients with pathological conditions are different from healthy subjects. Future work, by using DTT to study the anatomical details of the Meyer's loop in different kinds of pathologies involving the temporal lobe and to compare the differences between healthy subjects and patients may have potential important practical applications in preoperative planning for neurosurgical procedures and intraoperative guidance.

CONCLUSIONS

Our study presents a technique for demonstrating the Meyer's loop that showed a complex arrangement of the various projection fibers that compose the Meyer's loop and the intricate relations with the neighbouring fibers. These complex relations contribute to the challenges for an accurate demonstration of the Meyer's loop by DTT. An accurate appreciation of the Meyer's loop anatomical details by DTT may predict the postoperative VFD and may allow for surgical strategies and tactics to prevent injury to this structure during temporal resections for epilepsy.

REFERENCES

1. Türe U, Yaşargil MG, Friedman AH, Meftý Al O. Fiber dissection technique: lateral aspect of the brain. *Neurosurgery* 2000;47(2):417-26.
2. Yaşargil MG, Türe U, Yasargil DC. Impact of temporal lobe

CLINICAL ASPECTS

- surgery. *J. Neurosurg. American Association of Neurological Surgeons* 2004;101(5):725-38.
3. Goga C, Brinzaniuc K, Rodriguez-Mena R, Florian IS. The temporal lobe white matter fiber systems demonstrated by fiber dissection technique. *Romanian Journal of Functional and Clinical, Macro- and Microscopical Anatomy and Anthropology* 2014;13(1):7-15.
 4. Goga C, Brinzaniuc K, Florian IS, Rodriguez-Mena R. The three-dimensional architecture of the internal capsule of the human brain demonstrated by fiber dissection technique. *ARS Medica Tomitana* 2014;3(78):115-22.
 5. Basser PJ, Mattiello J, LeBihan D. MR diffusion tensor spectroscopy and imaging. *Biophys J* 1994;66:259-67.
 6. Basser PJ, Mattiello J, LeBihan D. Estimation of the effective self-diffusion tensor from the NMR spin echo. *J Magn Reson.* 1994;B 103:247-54.
 7. Basser PJ, Pajevic S, Pierpaoli C, Duda J, Aldroubi A. In vivo fiber tractography using DT-MRI data. *Magn Reson Med.* 2000;44:625-32.
 8. Conturo TE, Lori NF, Cull TS, Akbudak E, Snyder AZ, Shimony JS, et al. Tracking neuronal fiber pathways in the living human brain. *Proc Natl Acad Sci USA* 1999;96:10422-7.
 9. Jones DK. Studying connections in the living human brain with diffusion MRI. *Cortex* 2008;44:936-52.
 10. Mori S, van Zijl PC. Fiber tracking: principles and strategies—a technical review. *NMR Biomed* 2002;15:468-80.
 11. Yamamoto T, Yamada K, Nishimura T, Kinoshita S. Tractography to Depict Three Layers of Visual Field Trajectories to the Calcarine Gyri. *American Journal of Ophthalmology* 2005;140(5):781-1.
 12. Okada T, Miki Y, Kikuta K, Mikuni N, Urayama S, Fushimi Y. Diffusion tensor fiber tractography for arteriovenous: quantitative analyses to evaluate the corticospinal tract. *ANJR Am J Neuroradiol* 2007;28:1107-13.
 13. Ciccarelli O, Toosy AT, Hickman SJ, al E. Optic radiation changes after optic neuritis detected by tractography-based group mapping. *Hum Brain Mapp* 2005;25(3):308-16.
 14. Kikuta K, Takagi Y, Nozaki K, al E. Early experience with 3-T magnetic resonance tractography in the surgery of cerebral arteriovenous malformations in and around the visual pathways. *Neurosurgery* 2006;58:331-7.
 15. Powell HW, Parker GJ, Alexander DC, Symms MR, Boulby PA, Wheeler-Kingshott CA. MR tractography predicts visual field defects following temporal lobe resection. *Neurology* 2005;65:596-9.
 16. Taoka T, Sakamoto M, Nakagawa H, Nakase H, Iwasaki S, Takayama K, et al. Diffusion Tensor Tractography of the Meyer Loop in Cases of Temporal Lobe Resection for Temporal Lobe Epilepsy: Correlation between Postsurgical Visual Field Defect and Anterior Limit of Meyer Loop on Tractography. *American Journal of Neuroradiology* 2008;29(7):1329-34.
 17. Mori S, Kaufmann WE, Davatzikos C, Stieltjes B, Amodei L, al E. Imaging cortical association tracts in human brain. *Magn Reson Imag* 2002;47:215-23.
 18. Kovanlikaya I, Firat Z, Kovanlikaya A, Ulug AM, Cihangiroglu MM, John M, et al. Assessment of the corticospinal tract alterations before and after resection of brainstem lesions using diffusion tensor imaging (DTI) and tractography at 3T. *Eur J Radiol* 2011;77:383-91.
 19. Nilsson D, Starck G, Ljungberg M, Ribbelin S, Jönsson L, Malmgren K, et al. Intersubject variability in the anterior extent of the optic radiation assessed by tractography. *Epilepsy Research* 2007;77(1):11-6.
 20. Nieuwenhuys R, Voogd J, van Huijzen C. *The Human Central Nervous System*. 4 ed. Berlin: Springer-Verlag; 2008.
 21. Saeki N, Fujimoto N, Kubota M, Yamaura A. MR demonstration of partial lesions of the lateral geniculate body and its functional intra-nuclear topography. *Clin Neurol Neurosurg* 2003;106(1):28-32.
 22. Bjork A, Kugelberg E. Visual field defects after temporal lobectomy. *Acta Ophthalmol (Copenh)* 1957;35:210-6.
 23. Marino R Jr, Rasmussen T. Visual field changes after temporal lobectomy in man. *Neurology* 18(9):825-35.
 24. Penfield W. Temporal lobe epilepsy. *Br J Surg* 1954;41:337-43.
 25. Penfield W, Flanigin H. Surgical therapy for temporal lobe seizures. *Arch Neurol Psychiatry* 1950;64:490-500.
 26. Penfield W, Jasper H. *Epilepsy and Functional Anatomy of the Human Brain*. Boston: Little Brown; 1960.
 27. Rasmussen AT. The extent of recurrent geniculocalcarine fibers (loop of Archambault and Meyer) as demonstrated by gross brain dissection. *Anat Rec* 1943;85(3):277-84.
 28. Tecoma ES, Laxer KD, Barbaro NM. Frequency and characteristics of visual field defects after surgery for mesial temporal sclerosis. *Neurology* 1993;43:1235-8.
 29. Ebeling UU, Reulen HJ. Neurosurgical topography of the optic radiation. *Acta Neurochir* 1988;92(1-4):29-36.
 30. Choi C, Rubino PA, Fernández-Miranda JC, Abe H, Rhoton AL Jr. Meyer's loop and the optic radiations in the transylvian approach to the mediobasal temporal lobe. *Neurosurgery* 2006;59(4 Suppl 2):228-35.
 31. Choi C-Y, Han S-R, Yee G-T, Lee C-H. A Understanding of the Temporal Stem. *J Korean Neurosurg Soc* 2010;47(5):365-9.
 32. Párraga RG, Ribas GC, Welling LC, Alves RV, de Oliveira E. Microsurgical anatomy of the optic radiation and related fibers in 3-dimensional images. *Neurosurgery* 2012;71:160-72.
 33. Peltier J, Travers N, Destrieux C, Velut S. Optic radiations: a microsurgical anatomical study. *J. Neurosurg* 2006;105(2):294-300.
 34. Peltier J, Verclytte S, Delmaire C, Pruvo J-P, Godefroy O, Le Gars D. Microsurgical anatomy of the temporal stem: clinical relevance and correlations with diffusion tensor imaging fiber tracking. *J. Neurosurg* 2010;112(5):1033-8.
 35. Rubino PA, Rhoton AL Jr, Tong X, de Oliveira E. Three-dimensional relationships of the optic radiation. *Neurosurgery* 2005;57(Supplement 4):219-27.
 36. Krolak-Salmon P, Guenot M, Tiliket C, al E. Anatomy of the optic nerve radiations as assessed by static perimetry and MRI after tailored temporal lobectomy. *Br J Ophthalmol* 2000;84:884-9.
 37. Chen X, Weigel D, Ganslandt O, Buchfelder M, Nimsky C. Prediction of visual field deficits by diffusion imaging in temporal lobe epilepsy surgery. *NeuroImage* 2009;45:286-97.
 38. Thudium MO, Campos AR, Urbach H, Clusmann H. The Basal Temporal Approach for Mesial Temporal Surgery: Sparing the Meyer Loop with Navigated Diffusion Tensor Tractography. *Neurosurgery* 2010;67:ons385-90.
 39. Sherbondy AJ, Dougherty RF, Napel S, Wandell BA. Identifying the human optic radiation using diffusion tensor imaging and fiber tractography. *J Vis* 2008;8(10):12.1-12.11.
 40. Hofer S, Karaus A, Frahm. Reconstruction and dissection of the entire human visual pathway using diffusion tensor MRI. *Front Neuroanat* 2010;4:15.